JOURNAL OF PHYSICAL ORGANIC CHEMISTRY
J. Phys. Org. Chem. 2004; **17:** 138–147
Published online in Wiley InterScience (www.interscience.wiley.com). DOI: 10.1002/poc.704

Kinetics of the reactions between 1-fluoro-2,6-dinitrobenzene and pyrrolidine and piperidine in binary solvent systems: Influence of the nucleophile structure

P. M. Mancini,* G. G. Fortunato and L. R. Vottero

Departamento de Química, Área Química Orgánica, Facultad de Ingeniería Química, Universidad Nacional del Litoral, Santiago del Estero 2829, (3000) Santa Fe, Argentina

Received 26 May 2003; revised 15 July 2003; accepted 27 July 2003

ABSTRACT: We studied the kinetics of the reaction between 1-fluoro-2,6-dinitrobenzene and pyrrolidine or piperidine in ethyl acetate–chloroform or acetonitrile and acetonitrile–chloroform binary solvent mixtures. The kinetic response of these reactions was compared with that of the reactions with homopiperidine. The aim of this work was to evaluate the influence of the nucleophile structure and of solvent effects on those reactive systems. The amine structure has a great influence on second-order rate constants, especially on the rate constants related to the catalyzed step. In mixtures with chloroform the amine structure is also responsible for the change in the reaction mechanism. Theoretical quantum mechanics calculations confirm that the origin of these results lies in stereoelectronic effects due to the conformational difference between the amino moieties in the intermediate σ adducts as they release the nucleofuge. Solvation effects are dominated by non-specific interactions. The order of incidence of the molecular–microscopic solvent properties on the second-order rate coefficient k_A is dipolarity/polarizability > hydrogen-bond donor ability (HBD) > hydrogen-bond acceptor ability (HBA). The (HBA + HBD) and (HBA + HBA/HBD) solvent systems have similar solvation mechanisms: the critical state is preferentially solvated by the structure formed by intersolvent hydrogen-bonded species. Mixtures of the type (HBA/HBD + HBD) manifest a particular solvation behavior. Among the reactive systems selected there is only one example in which preferential solvation is not operative. Copyright © 2004 John Wiley & Sons, Ltd.
Additional material for this paper is available in Wiley Interscience

KEYWORDS: nucleophile structure; solvent effects; aromatic nucleophilic substitution; stereoelectronic effects; correlations; preferential solvation

INTRODUCTION

We have recently reported a study of the solvent effects on the kinetics of the nucleophilic aromatic substitution (S_NAr) reaction between 1-fluoro-2,6-dinitrobenzene (2,6-DNFB) and the secondary amine homopiperidine (HPIP) (hexahydro-1*H*-azepine), in ethyl acetate–chloroform or acetonitrile and acetonitrile–chloroform binary solvent mixtures.[1]

The mixed solvents chosen were representative of the types we proposed for mixtures of polar aprotic solvents where both pure solvents are able to form complexes or cross-associated species.[2,3] These mixtures were grouped on the basis of the molecular–microscopic descriptors determined in earlier measurements: type A [hydrogen-bond acceptor (HBA) solvent + potential hydrogen-bond donor (HBD) co-solvent]; type B [HBA solvent HBA/potential HBD co-solvent]; and type C [HBA/potential HBD solvent + potential HBD co-solvent].[3]

Here, we extended the analysis to the reactions between 2,6-DNFB and the secondary amines pyrrolidine (PYR) and piperidine (PIP), carried out in the solvent mixtures mentioned above.

The aims of this work were twofold: (i) to investigate the influence of solvent effects on the selected similar S_NAr processes performed in different mixed solvent systems; and (ii) to study the influence of the ring size of the nucleophile, comparing the kinetic response obtained by performing the reaction with the three homologous amines. In this direction, the corresponding results were analyzed in order to infer possible stereoelectronic effects related to the ring size of the cyclic amines used. Additionally, the kinetic results for the reactions with PYR and PIP carried out in binary mixtures of types A, B and C were evaluated and related through kinetic response patterns, multiparametric correlation analysis and preferential solvation models.

**Correspondence to:* P. M. Mancini, Departamento de Química, Área Química Orgánica, Facultad de Ingeniería Química, Universidad Nacional del Litoral, Santiago del Estero 2829, (3000) Santa Fe, Argentina.
E-mail: pmancini@fiqus.unl.edu.ar
Contract/grant sponsor: Science and Technology Secretariat, Universidad Nacional del Litoral; *Contract/grant numbers:* 2000-17-151; 2002-21-152; 2002-21-153.

Copyright © 2004 John Wiley & Sons, Ltd.

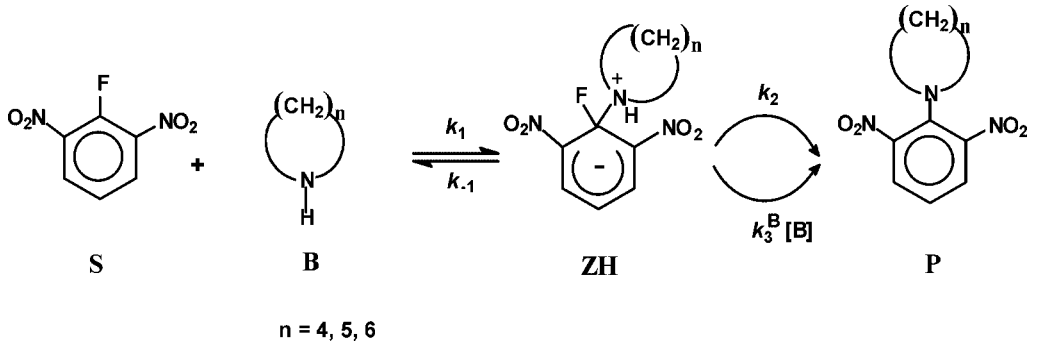

Scheme 1

RESULTS AND DISCUSSION

The kinetics of the S_NAr reactions between 2,6-DNFB and PYR and PIP respectively, in ethyl acetate (EAc)–$CHCl_3$, ethyl acetate and acetonitrile (AcN) and acetonitrile–$CHCl_3$ solvent systems were determined at 25 °C.

Kinetic results

The gross mechanism of S_NAr reactions when primary or secondary amines are the nucleophiles is now well established[4–6] (Scheme 1). In aprotic polar solvents, the reaction follows a second-order kinetic law represented by the equation

$$k_A = \frac{k_1\left(k_2 + k_3^B[B]\right)}{k_{-1} + k_2 + k_3^B[B]} \qquad (1)$$

Each reaction was explored at different solvent compositions, and the influence of amine concentration was studied in all cases. The reactions were carried out under pseudo-first-order conditions: they yielded the expected products in quantitative yield [*N*-(2,6-dinitrophenyl)pyrrolidine and *N*-(2,6-dinitrophenyl)piperidine], and proved to be first order in the corresponding substrate. The second-order rate constants, k_A, were calculated from the experimental pseudo-first-order rate constants k_φ and the appropriate amine concentration.

Reaction with PYR. Table S1 (Supporting Information, available at the epoc website at http://www.wiley.com/epoc) gives the k_A values for the reactions performed in the explored mixtures. The data in the pure solvents are additionally presented. For all solvent systems, the kinetic results reveal a satisfactory linear dependence of the rate on amine concentration, showing a zero intercept.

In order to understand the influence of the solvent effects on the explored reactions with changes in the composition of the mixtures, plots of k_A vs X_{CoS} at each amine concentration are presented in Fig. 1. The shapes of the curves for the reaction performed in EAc–$CHCl_3$ show a general pattern: the k_A values decrease from pure EAc to pure $CHCl_3$ as a non-linear function of the co-solvent molar fraction, exhibiting a negative deviation from the ideal response. The highest decrease takes place in HBD solvent-poor mixtures.

With respect to the reaction carried out in EAc–AcN mixtures, the plots also manifest a unique pattern of kinetic response: k_A increases with increase in the HBA/HBD solvent molar fraction over the whole range of amine concentration, exhibiting positive deviations from ideal behavior.

On the other hand, the reaction carried out in AcN–$CHCl_3$ shows a unique kinetic response pattern: k_A decreases with increase in the $CHCl_3$ molar fraction, exhibiting negative deviations from ideal response, as in the case of EAc–$CHCl_3$ mixtures. The highest decrease also takes place in HBD-poor mixtures.

Table S2 (Supporting Information) gives the k_1k_2/k_{-1} and k_1k_3/k_{-1} partial rate relations obtained by the linear regression treatment of the kinetic data. The k_1k_2/k_{-1} values are not statistically significant, so the reactions exhibit zero intercept and are clearly base-catalyzed in all solvent mixtures ($k_3/k_2 \gg 100$). The response of the k_1k_3/k_{-1} values can be considered approximately equivalent to that of the k_A values.

Reaction with PIP. Table S3 (Supporting Information) gives the k_A values for the reaction between 2,6-DNFB and PIP in the solvent systems explored, including the data in the pure solvents. As in the case for the reactions with PYR, in all instances the k_A second-order rate constant varies linearly with the amine concentration exhibiting zero intercept.

The plots of k_A vs X_{CoS} are shown in Fig. 1. The shapes of the curves for the reactions performed in EAc–$CHCl_3$ reveal two different kinetic responses depending on the co-solvent concentration. In the EAc-rich zone, the k_A values decrease with increase in the co-solvent molar fraction, giving rise to negative deviations, whereas in the $CHCl_3$-rich zone the kinetic response tends to an *ideal* behavior.

The reaction carried out in EAc–AcN mixtures manifests a unique pattern: the k_A values increase linearly with the HBA/HBD solvent molar fraction over the whole range of amine concentration, clearly yielding an ideal response.

Copyright © 2004 John Wiley & Sons, Ltd.

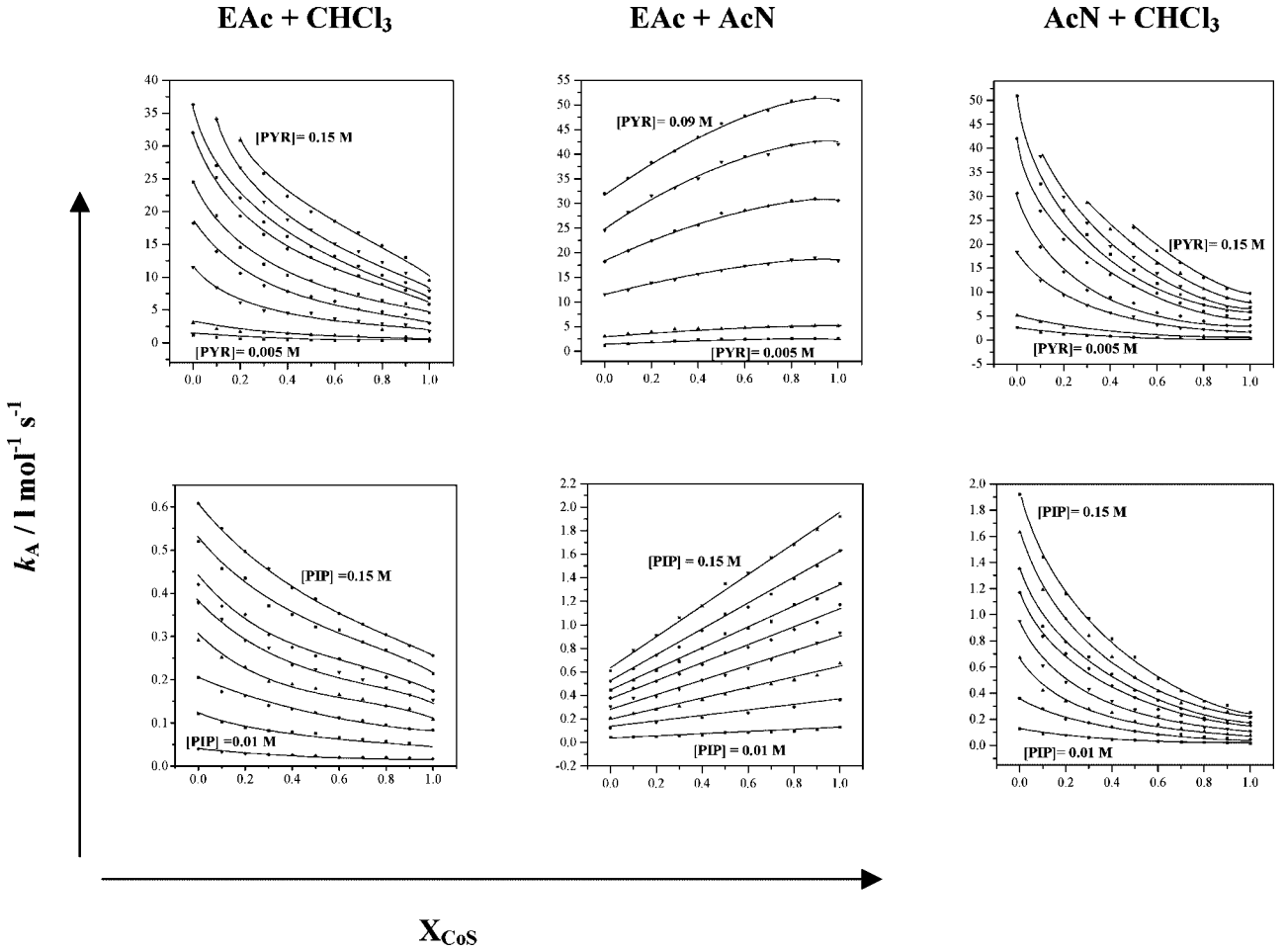

Figure 1. Plots of k_A vs X_{CoS} for the reaction of 2,6-DNFB with PYR or PIP in EAc–$CHCl_3$ or AcN and AcN–$CHCl_3$ mixtures, at each amine concentration

With respect to the reaction performed in AcN–$CHCl_3$, the shape of the curves is similar to that with the EAc–$CHCl_3$ mixtures: k_A decreases with increase in the co-solvent molar fraction, manifesting a negative deviation from ideal response, the highest decrease taking place in the HBD solvent-poor mixtures.

Table S4 (Supporting Information) gives partial rate relations k_1K_2/k_{-1} and k_1k_3/k_{-1} obtained by the linear regression treatment of the kinetic data. As in the case for the reactions with PYR, relations k_1k_2/k_{-1} are statistically not different from zero, which means that the reactions are highly base-catalyzed in all solvent mixtures ($k_3/k_2 \gg 100$).

The nucleophile influence

Comparison of amines. In order to achieve a comparative study of the homologous secondary amines PYR, PIP and HPIP, the kinetic data corresponding to PYR and PIP were compared with the previously reported data for HPIP.[1]

It is possible to estimate reactivity ratios $k_A^{PYR} : k_A^{PIP} : k_A^{HPIP}$ taking into account the k_A values for each amine with respect to HPIP in all binary solvent mixtures, at constant amine concentration.

Table 1 gives the corresponding relations at two amine concentrations (0.03 and 0.09 M) in the whole range of solvent composition and for all solvent systems.

The results corresponding to EAc–$CHCl_3$ mixtures suggest the following: (i) The amine with the smallest ring exhibits the highest rate. These ratios are higher in EAc-rich than in $CHCl_3$-rich mixtures. Thus, when the reactions are performed in the former mixtures, those with PYR are almost 300 times more reactive than those with HPIP; (ii) The $k_A^{PIP} : k_A^{HPIP}$ ratios decrease slightly with the co-solvent molar fraction and also indicate more similar rates for PIP and HPIP; (iii) The $k_A^{PYR} : k_A^{PIP}$ ratios also decrease with the co-solvent mole fraction and suggest that the five-membered ring amine is much more reactive than the six-membered ring amine. In EAc-rich mixtures, the reactions with PYR are almost 100 times more reactive than those with PIP.

The results corresponding to EAc–AcN binary mixtures suggest, as in the previous mixture, that the amine with the smallest ring exhibits the highest rate, but in this case the order of magnitude of the ratios remains constant with the co-solvent concentration.

Copyright © 2004 John Wiley & Sons, Ltd.

Table 1. Relations $k_A^{PYR} : k_A^{PIP} : k_A^{HPIP}$ and $k_A^{PYR} : k_A^{PIP}$ in binary solvent mixtures (including the data in the pure solvents)

		$k_A^{PYR} : k_A^{PIP} : k_A^{HPIP}$		$k_A^{PYR} : k_A^{PIP}$	
Solvent	X_{CoS}	[Amine] = 0.03 M	[Amine] = 0.09 M	[Amine] = 0.03 M	[Amine] = 0.09 M
EAc		303 : 3.18 : 1	280 : 3.30 : 1	95 : 1	85 : 1
AcN		238 : 4.70 : 1	236 : 5.44 : 1	51 : 1	43 : 1
$CHCl_3$		47.6 : 1.16 : 1	87 : 2.30 : 1	41 : 1	38 : 1
EAc–$CHCl_3$	0.1	300 : 3.68 : 1	240 : 3.20 : 1	81 : 1	74 : 1
EAc–AcN		318 : 4.10 : 1	292 : 3.80 : 1	76 : 1	76 : 1
AcN–$CHCl_3$		182 : 4.10 : 1	188 : 4.90 : 1	44 : 1	39 : 1
EAc–$CHCl_3$	0.2	236 : 3.42 : 1	201 : 3.00 : 1	69 : 1	66 : 1
EAc–AcN		356 : 4.30 : 1	314 : 4.26 : 1	82 : 1	74 : 1
AcN–$CHCl_3$		170 : 3.60 : 1	189 : 4.90 : 1	47 : 1	38 : 1
EAc–$CHCl_3$	0.3	212 : 3.56 : 1	185 : 3.07 : 1	59 : 1	60 : 1
EAc–AcN		632 : 5.00 : 1	325 : 4.64 : 1	72 : 1	70 : 1
AcN–$CHCl_3$		151 : 3.60 : 1	185 : 4.90 : 1	42 : 1	37 : 1
EAc–$CHCl_3$	0.4	206 : 3.69 : 1	164 : 2.70 : 1	57 : 1	61 : 1
EAc–AcN		371 : 5.00 : 1	334 : 5.10 : 1	74 : 1	66 : 1
AcN–$CHCl_3$		124 : 3.00 : 1	172 : 4.40 : 1	41 : 1	39 : 1
EAc–$CHCl_3$	0.5	188 : 3.17 : 1	157 : 2.70 : 1	59 : 1	58 : 1
EAc–AcN		356 : 5.40 : 1	340 : 5.60 : 1	66 : 1	61 : 1
AcN–$CHCl_3$		112 : 2.20 : 1	149 : 3.70 : 1	39 : 1	40 : 1
EAc–$CHCl_3$	0.6	154 : 2.79 : 1	139 : 2.70 : 1	55 : 1	52 : 1
EAc–AcN		353 : 5.10 : 1	318 : 5.40 : 1	69 : 1	59 : 1
AcN–$CHCl_3$		86 : 5.10 : 1	137 : 3.20 : 1	69 : 1	43 : 1
EAc–$CHCl_3$	0.7	118 : 2.18 : 1	127 : 2.70 : 1	54 : 1	51 : 1
EAc–AcN		316 : 5.30 : 1	294 : 5.24 : 1	60 : 1	56 : 1
AcN–$CHCl_3$		72 : 2.40 : 1	119 : 2.90 : 1	30 : 1	41 : 1
EAc–$CHCl_3$	0.8	94.8 : 1.84 : 1	114 : 2.30 : 1	51 : 1	49 : 1
EAc–AcN		308 : 5.00 : 1	282 : 5.33 : 1	62 : 1	53 : 1
AcN–$CHCl_3$		71 : 2.10 : 1	107 : 2.90 : 1	34 : 1	43 : 1
EAc–$CHCl_3$	0.9	86 : 1.65 : 1	107 : 2.20 : 1	52 : 1	48 : 1
EAc–AcN		279 : 5.00 : 1	264 : 5.23 : 1	56 : 1	50 : 1
AcN–$CHCl_3$		63 : 1.96 : 1	96 : 2.60 : 1	32 : 1	36 : 1

The relations obtained for AcN–$CHCl_3$ mixtures allowed us to arrive at conclusions similar to those obtained for EAc–$CHCl_3$ mixtures.

In order to compare the constants corresponding to the $k_1k_3/k_{-1}(k^{AMINE})$ catalyzed pathway, relations $k^{PYR} : k^{PIP} : k^{HPIP}$ were calculated for all solvent systems (Table 2). The results reveal a high incidence of the amine structure in the catalyzed step, which is favored by the amine with the smallest ring. The corresponding relations were calculated for the reactions between these amines and 1-fluoro-2,4-dinitrobenzene,[7] arriving at equivalent conclusions. These results can be related to stereoelectronic effects and to conformational differences depending on the ring size of the amine.

Influence of the cyclic amine on the catalyzed pathway: theoretical calculations. With a view to explaining the remarkable differences in rates between the cyclic amines specially related to the rate constants on the catalyzed pathway, and in order to confirm whether the ring size of the amine plays a role in that step, semiempirical molecular orbital calculations at the AM1 (Austin Model 1)[8] level were carried out in a vacuum with the HyperChem 5.11 systems of programs.

Such huge differences, specifically between PYR and PIP, were found in similar systems and they were ascribed to conformational or stereoelectronic effects in the transition state leading to the reaction product.[9] It was suggested that the unshared electron pair on the amine-nitrogen of the anionic σ intermediate (Z^-) must be antiperiplanar with respect to the rupturing C—F bond in the transition state, making it possible that the amino moiety approaches a coplanar geometry, which is a canonical form of the product. Related to this, it was also suggested that the carbon-bound amino moiety in the transition state for that step should be intermediate between its conformations in Z^- (antiperiplanar conformation) and in the canonical structure. The structure **I** is the respective canonical form of the product corresponding to our reactive system.

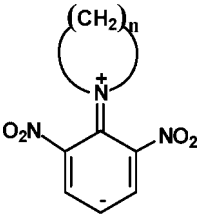

(I)

If we consider that the SB–GA (Specific Base–General Acid) mechanism is operative for the ZH intermediate

Copyright © 2004 John Wiley & Sons, Ltd.

Table 2. Relations $k^{PYR} : k^{PIP} : k^{HPIP}$ and $k^{PYR} : k^{PIP}$ in binary solvent mixtures (including the data in the pure solvents)

Solvent	X_{CoS}	$k_A^{PYR} : k_A^{PIP} : k^{HPIP}$	$k_A^{PYR} : k_A^{PIP}$
EAc		294 : 3.35 : 1	88 : 1
AcN		284 : 6.30 : 1	45 : 1
$CHCl_3$		140 : 3.75 : 1	37 : 1
EAc–$CHCl_3$	0.1	239 : 3.25 : 1	73 : 1
EAc–AcN		305 : 3.97 : 1	77 : 1
AcN–$CHCl_3$		217 : 5.60 : 1	39 : 1
EAc–$CHCl_3$	0.2	198 : 3.21 : 1	62 : 1
EAc–AcN		326 : 4.70 : 1	70 : 1
AcN–$CHCl_3$		219 : 6.00 : 1	36 : 1
EAc–$CHCl_3$	0.3	181 : 3.16 : 1	57 : 1
EAc–AcN		329 : 5.06 : 1	65 : 1
AcN–$CHCl_3$		231 : 6.90 : 1	33 : 1
EAc–$CHCl_3$	0.4	160 : 2.93 : 1	55 : 1
EAc–AcN		344 : 5.55 : 1	62 : 1
AcN–$CHCl_3$		208 : 6.10 : 1	34 : 1
EAc–$CHCl_3$	0.5	162 : 3.05 : 1	53 : 1
EAc–AcN		370 : 6.30 : 1	58 : 1
AcN–$CHCl_3$		197 : 5.50 : 1	36 : 1
EAc–$CHCl_3$	0.6	149 : 2.96 : 1	50 : 1
EAc–AcN		352 : 6.20 : 1	56 : 1
AcN–$CHCl_3$		184 : 4.90 : 1	38 : 1
EAc–$CHCl_3$	0.7	148 : 2.96 : 1	50 : 1
EAc–AcN		329 : 6.20 : 1	53 : 1
AcN–$CHCl_3$		176 : 4.30 : 1	41 : 1
EAc–$CHCl_3$	0.8	145 : 3.05 : 1	48 : 1
EAc–AcN		318 : 6.30 : 1	51 : 1
AcN–$CHCl_3$		152 : 3.90 : 1	39 : 1
EAc–$CHCl_3$	0.9	139 : 3.07 : 1	45 : 1
EAc–AcN		303 : 6.30 : 1	48 : 1
AcN–$CHCl_3$		127 : 3.60 : 1	35 : 1

decomposition step, the k_1k_3/k_{-1} constants relative to this pathway are equivalent in this case to the product of the first equilibrium constant (K_1), the acid dissociation constant of the zwiterionic intermediate (K_3), and the specific rate constant for the general acid-catalyzed nucleofuge departure (k_4) (Scheme 2). It can be assumed

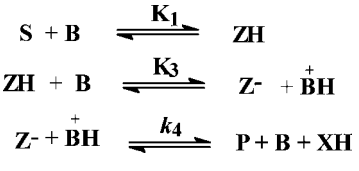

Scheme 2

that the kinetic differences between the three cyclic amines do not arise from the first equilibrium (K_1)[9,10] and provided they have pK_a[11] values that do not differ greatly, the same acidity for the ZH intermediates can be considered. The previous considerations would imply that the differences in the k_1k_3/k_{-1} parameter must stem from a difference in the k_4 values. As a consequence, the ring size of the amine would play a critical role in the transition state for the separation of the fluorine atom from the Z^- intermediate.

In this direction, the Z^- σ-complexes intermediate geometric structures for PYR, PIP and HPIP were optimized at the AM1 level. From the structures which represent a local minimum in the potential energy surface, it was possible to determine the total energy (E_T), the heat of formation (ΔH) and the heat of formation with respect to reactants ($\Delta\Delta H_{Reactants}$) (Table 3). Total energies and heats of formation corresponding to reactants (substrate and cyclic amines) are given as Supporting Information (Table S5). The negative values obtained for $\Delta\Delta H_{Reactants}$ indicate that the formation of these complexes for all amines is exothermic. In order to analyze the antiperiplanar Z^- conformations for all intermediates, a conformational search was carried out [based on the rotation of a dihedral angle formed by the C_{ipso}—N (amino group) bond, the C_{ipso}—F bond and the N—C_α bond of the amino moiety]. The respective energies are listed in Table 3. The structures obtained are shown in Figs S1–S3 (Supporting Information). The conformational search yielded only one antiperiplanar conformation for PYR and two conformations for PIP and HPIP. In order to compare the energy between these structures and those previously optimized, the magnitude of ΔE was calculated. This value represents the difference in the ΔH values between the structure corresponding to an energy minimum and the antiperiplanar conformation. It can be clearly appreciated that both conformations derived from PYR are equivalent ($\Delta E = 0$), whereas for PIP and HPIP derivatives the antiperiplanar conformations correspond to structures energetically higher than those which constitute a local minimum. This means that reaching the corresponding antiperiplanar conformation in order to evolve to the transition state would be easier for PYR than for PIP and HPIP intermediates.

Table 3. Total energy and heats of formation at AM1 level corresponding to Z^- intermediates[a]

	Z^- conformation	E_T (kcal mol^{-1})	ΔH (kcal mol^{-1})	$\Delta\Delta H_{Reactants}$ (kcal mol^{-1})	ΔE (kcal mol^{-1})
2,6-DNFB + PYR	Minimum energy	−87973.8	−59.80	−43.64	
	Antiperiplanar	−87973.8	−59.80		0
2,6-DNFB + PIP	Minimum energy	−91568.08	−67.25	−39.71	
	Antiperiplanar	−91568.08	−67.25		0
		−91567.52	−66.68		0.57
2,6-DNFB + HPIP	Minimum energy	−95156.97	−69.30	−38.68	
	Antiperiplanar	−95156.65	−69.00		0.30
		−95156.30	−68.72		0.58

[a] E_T, total energy; ΔH, heat of formation; $\Delta\Delta H_{Reactant}$, heat of formation with respect to reactants; ΔE, heat of formation difference between the minimum energy and the antiperiplanar conformations. 1 kcal = 4.184 kJ.

Copyright © 2004 John Wiley & Sons, Ltd.

Table 4. Total energy and heats of formation at AM1 level corresponding to product minimum energy and to canonical structures

	Product structure	E_T (kcal mol^{-1})	ΔH (kcal mol^{-1})	$\Delta\Delta H_{Reactants}$ (kcal mol^{-1})	$\Delta\Delta H_{Products}$ (kcal mol^{-1})	$\Delta\Delta H_{Z^-}$ (kcal mol^{-1})
2,6-DNFB + PYR	Minimum energy	−76730.03	42.96	59.12		
	Canonical structure	−76729.15	43.84	59.99	0.884	103.6
2,6-DNFB + PIP	Minimum energy	−80326.11	33.72	61.26		
	Canonical structure	−80319.43	40.40	67.94	6.680	107.1
2,6-DNFB + HPIP	Minimum energy	−83916.23	30.43	61.05		
	Canonical structure	−83904.60	41.82	72.44	11.39	110.5

In order to evaluate the possibility that the carbon-bound amino moiety in the transition state approaches a coplanar geometry, the respective products and structures of type **I** were optimized at AM1 level for each amino derivatives. As expected, the optimized product structures [Figs S4(a), S5(a) and S6(a), Supporting Information] obtained for the three amines do not exhibit that coplanar geometry, and the corresponding structures of type **I** [Figs S4(b), S5(b) and S6(b), Supporting Information] with the carbon-bound amino moiety coplanar are energetically higher than the former. Table 4 shows the resultant energies for all structures. The positive values obtained for $\Delta\Delta H_{Reactants}$ indicate that the formation of the products for all amines is endothermic. This allows us to make some suggestions about the respective transition states taking into account the product structures. In this direction, the trends observed for the ΔH values of canonical structures with respect to products ($\Delta\Delta H_{Product}$) and with respect to antiperiplanar Z^- conformations ($\Delta\Delta H_{Z^-}$) indicate that the structures in the transition state derived from the amine with the smallest ring are energetically favored to approach the coplanar geometry necessary to progress towards products.

The previous results show that the origin of the differential behaviors lies in special conformations related to the ring size of the amine.

The solvent influence

Correlation analysis of kinetic data with molecular–microscopic solvent properties: solvent effects on the second-order rate coefficient k_A. The kinetic data and the molecular–microscopic solvent properties were correlated by means of a multiparametric approach in order to interpret quantitatively the influence of the solvent effects on the explored reactions. The chosen multiparametric equation was that developed by Kamlet *et al.*:[12]

$$\log k_A = Y + s\pi^* + a\alpha + b\beta \qquad (2)$$

where s, a and b measure the relative susceptibilities of the reactive system with respect to the solvent properties (dipolarity/polarizability, HBD and HBA ability). This treatment allowed us to determine the incidence of each type of solvent property on the kinetics of the reaction. The results obtained from this correlation are presented in Tables 5 and 6, corresponding to the reactions with PYR and PIP, respectively.

The good correlations obtained by multiple regression analysis (based on least squares) over the whole range of solvent compositions allow an interpretation of the influence of any mixed solvent property on the kinetic process.

For the system with PYR, the coefficient b is, in most cases, not statistically significant at the 90% confidence level, or higher, according to Student's t-test. In EAc–$CHCl_3$ mixtures coefficients s and a are negative at all amine concentrations, which means that an increase in the dipolarity/polarizability and in the HBD ability of the mixed solvent decreases the k_A values. Considering the magnitude of the s and a coefficients for these correlations, it can be inferred that the k_A values are more sensitive to dipolarity/polarizability than to the HBD ability, resulting in $3.3 < s/a < 6.8$. In AcN–$CHCl_3$ mixtures the coefficients s are also negative but the coefficients a are positive at all amine concentrations. As in the previous system, the dipolarity/polarizability of the solvent has a greater effect on the k_A values than the HBD ability ($3.2 < s/a < 5.8$). For the reaction performed in EAc–AcN mixtures, the coefficient s is not statistically significant, the k_A values being linearly dependent on the HBD ability of the solvent, thus $\log k_A = Y + a\alpha$.

For the system with PIP, in EAc–$CHCl_3$ mixtures, the coefficients s, a and b are negative and their magnitudes follow the order $s > a \approx b$, thus $4.7 < s/a < 8.8$, $6.0 < s/b < 10$. It must be pointed out that for some amine concentrations, the coefficients a and b are not statistically significant. In AcN–$CHCl_3$, the correlation gives negative values for coefficients s and positive values for coefficients a and b, their order of incidence being $s > a > b$, thus $2.1 < s/a < 4.7$, $7.0 < s/b < 13$, $1.5 < a/b < 6.1$. It can be clearly seen that the systems are also very sensitive to the dipolarity/polarizability of the solvent. With respect to the EAc–AcN mixtures, the reactive system is sensitive to dipolarity/polarizability in addition to the HBD ability of the solvent ($1.1 < s/a < 1.7$). The coefficient b is not statistically significant at the 90% or higher confidence level at most amine concentrations.

Copyright © 2004 John Wiley & Sons, Ltd.

Table 5. Correlation coefficient (r and r^2), standard deviation (SD), intercept (Y) and the parameters s, a, and b (and their standard errors) and the number of data points (n) corresponding to log $k_A = Y + s\pi^* + a\alpha + b\beta$ for the reaction between 2,6-DNFB and PYR in binary mixtures (including the data in pure solvents)

Solvent	[PYR](M)	r (r^2)	SD	Y (s_Y)	s (s_s)	a (s_a)	b (s_b)	n
EAc–$CHCl_3$	0.005	0.975 (0.951)	0.048	+2.220 (0.398)	−3.522 (0.456)	−1.079 (0.233)	−0.479 (0.336)	11
	0.01	0.978 (0.957)	0.050	+2.415 (0.411)	−3.410 (0.473)	−0.814 (0.242)	−0.151 (0.348)	11
	0.03	0.973 (0.946)	0.064	+3.552 (0.525)	−4.175 (0.602)	−0.875 (0.308)	−0.449 (0.443)	11
	0.05	0.967 (0.935)	0.070	+3.942 (0.581)	−4.359 (0.666)	−0.685 (0.341)	−0.665 (0.490)	11
	0.07	0.974 (0.949)	0.060	+4.281 (0.497)	−4.527 (0.570)	−0.703 (0.291)	−0.914 (0.419)	11
	0.09	0.976 (0.952)	0.057	+4.155 (0.472)	−4.252 (0.542)	−0.624 (0.277)	−0.717 (0.398)	11
	0.1	0.975 (0.950)	0.057	+4.061 (0.470)	−4.061 (0.539)	−0.655 (0.275)	−0.629 (0.396)	11
	0.125	0.978 (0.956)	0.056	+4.345 (0.459)	−4.329 (0.527)	−0.727 (0.269)	−0.713 (0.387)	11
	0.150	0.976 (0.952)	0.057	+4.315 (0.474)	−4.201 (0.543)	−0.762 (0.278)	−0.628 (0.400)	11
EAc–AcN	0.005	0.989 (0.978)	0.020	−0.819 (0.558)	+0.617 (0.523)	+0.734 (0.281)	+1.159 (0.607)	11
	0.01	0.987 (0.974)	0.014	+0.025 (0.390)	+0.444 (0.366)	+0.437 (0.197)	+0.447 (0.424)	11
	0.03	0.984 (0.969)	0.015	+0.741 (0.425)	+0.517 (0.398)	+0.381 (0.214)	+0.04 (0.461)	11
	0.05	0.991 (0.981)	0.013	+1.133 (0.354)	+0.288 (0.332)	+0.559 (0.178)	−0.094 (0.384)	11
	0.07	0.992 (0.985)	0.011	+0.971 (0.317)	+0.533 (0.297)	+0.436 (0.160)	+0.249 (0.344)	11
	0.09	0.990 (0.981)	0.012	+1.378 (0.324)	+0.304 (0.303)	+0.476 (0.163)	−0.115 (0.352)	11
AcN–$CHCl_3$	0.005	0.993 (0.986)	0.042	+5.122 (0.757)	−7.197 (0.972)	+1.241 (0.245)	+0.626 (0.231)	11
	0.01	0.982 (0.965)	0.070	+4.880 (1.256)	−6.526 (1.513)	+1.433 (0.407)	+0.547 (0.384)	11
	0.03	0.993 (0.987)	0.047	+5.042 (0.855)	−6.170 (1.099)	+1.815 (0.277)	+0.522 (0.261)	11
	0.05	0.986 (0.972)	0.065	+5.667 (1.178)	−6.687 (1.513)	+1.404 (0.382)	+0.776 (0.360)	11
	0.07	0.987 (0.974)	0.060	+5.104 (1.076)	−5.719 (1.383)	+1.405 (0.349)	+0.687 (0.329)	11
	0.09	0.988 (0.977)	0.055	+4.526 (0.997)	−4.839 (1.281)	+1.661 (0.323)	+0.465 (0.305)	11
	0.1	0.985 (0.970)	0.063	+4.681 (1.139)	−4.957 (1.463)	+1.567 (0.369)	+0.519 (0.348)	11

Preferential solvation effects on kinetic results: application of preferential solvation models. In order to obtain information about the solvation effects on the reagents and/or intermediates of the explored S_NAr reaction, we applied the general equation based on solvent exchange theory by Bosh and co-workers:[13]

$$Y = Y_1 + \frac{f_{2/1}(Y_2 - Y_1)\left(x_2^0\right)^2 + f_{12/1}(Y_{12} - Y_1)\left(1 - x_2^0\right)x_2^0}{\left(1 - x_2^0\right)^2 + f_{2/1}\left(x_2^0\right)^2 + f_{12/1}\left(1 - x_2^0\right)x_2^0} \quad (3)$$

The application of this preferential solvation model to the k_A values in the whole range of solvent composition allowed us to determine the corresponding preferential solvation parameters $f_{2/1}$ and $f_{12/1}$, which measure the tendency of the solutes to be solvated by co-solvent S2 and by the 'mixed solvent' S12 (structure attributed to the formation of intersolvent complexes or associates by hydrogen-bond interactions) with reference to solvent S1. The corresponding results are presented in Table S6 (Supporting Information).

For the reactions with PYR performed in EAc–$CHCl_3$ mixtures, at all amine concentrations it can be seen that: (i) $f_{2/1} < 1$, indicating that the preferential solvation is produced by EAc in preference to $CHCl_3$; (ii) $f_{12/1} > 1$, suggesting preferential solvation by S12 in preference to EAc and $CHCl_3$. As a consequence, the preferential

Copyright © 2004 John Wiley & Sons, Ltd.

Table 6. Correlation coefficient (r and r^2), standard deviation (SD), intercept (Y) and the parameters s, a, and b (and their standard errors) and the number of data points (n) corresponding to log $k_A = Y + s\pi^* + a\alpha + b\beta$ for the reaction between 2,6-DNFB and PIP in binary mixtures (including the data in pure solvents)

Solvent	[PIP] (M)	r (r^2)	SD	Y (s_Y)	s (s_s)	a (s_a)	b (s_b)	n
EAc–$CHCl_3$	0.01	0.980 (0.960)	0.027	+0.175 (0.198)	−2.488 (0.246)	−0.531 (0.133)	−0.414 (0.134)	11
	0.03	0.971 (0.944)	0.037	+0.542 (0.271)	−2.450 (0.336)	−0.404 (0.182)	−0.227 (0.183)	11
	0.05	0.970 (0.941)	0.037	+1.020 (0.267)	−2.700 (0.332)	−0.379 (0.179)	−0.473 (0.180)	11
	0.07	0.972 (0.945)	0.036	+0.910 (0.260)	−2.407 (0.323)	−0.410 (0.175)	−0.238 (0.176)	11
	0.09	0.965 (0.931)	0.039	+1.201 (0.287)	−2.590 (0.357)	−0.382 (0.193)	−0.408 (0.194)	11
	0.1	0.963 (0.928)	0.039	+1.156 (0.283)	−2.459 (0.351)	−0.342 (0.191)	−0.369 (0.191)	11
	0.125	0.967 (0.935)	0.036	+1.131 (0.263)	−2.311 (0.326)	−0.332 (0.177)	−0.290 (0.177)	11
	0.150	0.978 (0.956)	0.034	+1.379 (0.247)	−2.530 (0.306)	−0.287 (0.166)	−0.423 (0.166)	11
EAc–AcN	0.01	0.989 (0.978)	0.027	−0.787 (0.753)	+0.585 (0.706)	+0.978 (0.380)	−2.019 (0.818)	11
	0.03	0.994 (0.989)	0.018	−1.492 (0.508)	+1.171 (0.477)	+0.680 (0.257)	−0.177 (0.552)	11
	0.05	0.996 (0.992)	0.018	−0.818 (0.493)	+0.991 (0.462)	+0.888 (0.249)	−0.963 (0.535)	11
	0.07	0.996 (0.993)	0.015	−0.449 (0.429)	+0.823 (0.402)	+0.905 (0.216)	−1.174 (0.466)	11
	0.09	0.998 (0.997)	0.010	−0.748 (0.283)	+1.076 (0.266)	+0.776 (0.143)	−0.628 (0.308)	11
	0.1	0.997 (0.995)	0.013	−0.578 (0.365)	+0.941 (0.343)	+0.881 (0.184)	−0.693 (0.352)	11
	0.125	0.997 (0.995)	0.015	−0.847 (0.419)	+1.280 (0.393)	+0.734 (0.211)	−0.366 (0.456)	11
	0.150	0.998 (0.997)	0.011	−0.798 (0.300)	+1.121 (0.281)	+0.841 (0.151)	−0.121 (0.326)	11
AcN–$CHCl_3$	0.01	0.995 (0.991)	0.034	+2.740 (0.613)	−5.857 (0.788)	+1.237 (0.199)	+0.807 (0.187)	11
	0.03	0.992 (0.984)	0.045	+2.973 (0.804)	−5.571 (1.033)	+1.265 (0.260)	+0.790 (0.246)	11
	0.05	0.990 (0.980)	0.051	+3.137 (0.916)	−5.484 (1.177)	+1.361 (0.297)	+0.709 (0.280)	11
	0.07	0.989 (0.978)	0.054	+2.888 (0.975)	−4.958 (1.253)	+1.572 (0.316)	+0.536 (0.298)	11
	0.09	0.995 (0.991)	0.033	+2.848 (0.596)	−4.708 (0.766)	+1.639 (0.193)	+0.419 (0.182)	11
	0.1	0.991 (0.982)	0.047	+2.255 (0.853)	−3.879 (1.096)	+1.798 (0.276)	+0.293 (0.260)	11
	0.125	0.995 (0.991)	0.032	+2.899 (0.585)	−4.584 (0.751)	+1.589 (0.1889)	+0.462 (0.179)	11
	0.150	0.995 (0.990)	0.035	2.748 (0.633)	−4.301 (0.813)	+1.559 (0.205)	+0.550 (0.193)	11

solvation order is intersolvent complex > EAc > $CHCl_3$. The results in EAc–AcN mixtures indicate in general the same preferential solvation order corresponding to EAc–$CHCl_3$: intersolvent complex > EAc > AcN. On the other hand, in AcN–$CHCl_3$ mixtures the observed preferential solvation order is $CHCl_3$ > intersolvent complex > AcN.

For the reactions with PIP carried out in EAc–$CHCl_3$ mixtures, the preferential solvation order at most amine concentrations is intersolvent complex > EAc > $CHCl_3$. With respect to AcN–$CHCl_3$ mixtures, as in the case of the reactions with PYR, the critical state of the reaction is preferentially solvated by the co-solvent with HBD ability, AcN being the least preferred solvent.

As has been argued, considering the linear kinetic response observed in EAc–AcN mixtures, the reactive system constitutes, at first sight, an ideal system. In this case, Eqn (3) reduces to

$$Y = x_1^0 Y_1 + x_2^0 Y_2 \quad (4)$$

Copyright © 2004 John Wiley & Sons, Ltd.

Table 7. Linear regression treatment of the k_A values (Table S3) vs X_{AcN} for each amine concentration, corresponding to the reaction between 2,6-DNFB and PIP in EAc–AcN mixtures; intercept k_{EAc} (standard error *s*) and slope ($k_{AcN}-k_{EAc}$) (standard error *s*) according to Eqn (7)

[PIP] M	Intercept (*s*)	Slope (*s*)	*r*	SD	*n*	k_{EAc}	$k_{AcN}-k_{EAc}$
0.01	0.036 (0.003)	0.081 (0.005)	0.977	0.006	11	0.040	0.088
0.03	0.126 (0.005)	0.230 (0.009)	0.993	0.009	11	0.121	0.239
0.05	0.190 (0.010)	0.441 (0.017)	0.993	0.018	11	0.205	0.465
0.07	0.284 (0.012)	0.613 (0.020)	0.995	0.021	11	0.291	0.659
0.09	0.369 (0.013)	0.750 (0.022)	0.996	0.023	11	0.378	0.792
0.1	0.438 (0.012)	0.893 (0.021)	0.998	0.022	11	0.420	0.930
0.125	0.510 (0.011)	1.100 (0.018)	0.999	0.019	11	0.520	1.110
0.150	0.649 (0.015)	1.299 (0.025)	0.998	0.026	11	0.608	1.310

which implies a linear relation between the kinetic property and the solvent composition. As a consequence, it would imply that there is no preferential solvation and the corresponding property of the mixed solvent is the simple average of these properties in the pure solvents. Applying the corresponding equation to the kinetic data in EAc–AcN mixtures and as a function of X_{AcN}, it becomes

$$k_A = X_{EAc}k_{EAc} + X_{AcN}k_{AcN} = k_{EAc} + (k_{AcN} - k_{EAc})X_{AcN} \quad (5)$$

where k_A is the second-order rate constant for a defined composition of the mixture, and k_{EAc} and k_{AcN} are the corresponding parameters in the pure solvents.

In order to establish if the experimental data satisfy Eqn (5), linear regression analysis was applied to the lines obtained from the k_A vs X_{AcN} pattern (Fig. 1) at each amine concentration. The results are shown in Table 7. The good correlation coefficients and the probability $P < 0.0001$ indicate a linear relationship between k_A and X_{AcN}. The intercept and slope resulting from the linear regression analysis at each amine concentration were compared with the experimental k_{EAc} and $k_{AcN} - k_{EAc}$ values (Table 7). The good agreement obtained allow us to confirm that the experimental data satisfy Eqn (5), so the 2,6-DNFB–PIP/EAc–AcN reactive system constitutes an ideal system.

CONCLUSIONS

This comparative study related to the influence of the amine structure and solvent effects on the selected reactive systems allow us to conclude the following.

1. The kinetic results corresponding to the reactions with PYR and PIP reveal that there is no significant contribution to k_A from the spontaneous pathway for the decomposition of the zwitterionic intermediate, the reactions going exclusively via the base-catalyzed pathway. It may be argued that, in these reactive systems, the HBD solvents cannot effectively assist the fluoride detachment. In contrast, in reactions with HPIP the constants related to the non-catalyzed step are significant. This behavior can be related to stereoelectronic effects that come into play during the catalyzed step.
2. The amine with the smallest ring size exhibits huge differences in rates with respect to the rest of the amines. Those differences are more pronounced when the reaction is carried out in HBA solvent-rich mixtures.
3. The nucleophile structure has a great influence in the catalyzed pathway, being also greater in solvents with high HBA ability. The smaller the ring size of the nucleophile, the more effective is its catalytic power.
4. Theoretical quantum mechanics calculations show that the origin of previous behavior lies in stereoelectronic effects which come into play during the nucleofuge departure. These effects are forced by differences in conformation related to the ring size of the amine. The conformational difference is more crucial between PYR and PIP and/or PYR and HPIP than between PIP and HPIP.
5. The nucleophile structure is also responsible for the change in reaction mechanism in mixtures with $CHCl_3$: while the reactions with PYR and PIP are catalyzed in the whole range of co-solvent concentration, those with HPIP are non-catalyzed in HBD-rich mixtures.
6. In all reactive systems, the rate constant is more susceptible to solvent effects related to dipole and induced-dipole interactions than those attributed to hydrogen-bond interactions. Hence the solvation effects are dominated by non-specific interactions.

   Exceptions are the reactive systems 2,6-DNFB + HPIP[1] in EAc–$CHCl_3$ at low amine concentrations (for which the kinetic retarding effect takes place) and 2,6-DNFB + PYR/PIP in EAc + AcN. These systems are dominated by specific interactions related to the HBD ability of the solvent.

   The incidence of the solvation effects ascribed to the HBA solvent properties has little influence in all cases.
7. If we consider the solvatochromic response patterns (solvatochromic property vs X_{CoS}), the EAc–$CHCl_3$ mixtures exhibit synergism for α, a negative deviation from ideality for π^* and a positive deviation for

Copyright © 2004 John Wiley & Sons, Ltd.

β.[14a] The kinetic response patterns of k_A values vs X_{CoS} corresponding to the three nucleophiles are characterized by exhibiting negative deviations from the ideal response, π^* being the dominant solvent property. On the other hand, the EAc–AcN mixtures exhibit a nearly linear response for π^*, positive deviations for α and a small synergism for β.[14b] The corresponding kinetic response patterns of k_A values show positive deviations from the ideal response in reactions with PYR, for which α is dominant, and an ideal response in reactions with PIP, which are dominated by π^* and α properties. Finally, the solvatochromic response for AcN–$CHCl_3$ mixtures is characterized by a small synergism for π^* and positive deviations for α and β.[14a] The corresponding kinetic response exhibits negative deviations from ideal behavior, π^* being the dominant solvent property as in the case of EAc–$CHCl_3$ mixtures.

The above considerations allow us to conclude that for solvent systems A (HBA + HBD) and B (HBA + HBA/HBD), the solvatochromic process and the kinetic process are related to each other. This correspondence might come from similar solvation mechanisms.

8. The previous assumption is confirmed by the application of the preferential solvation model to the kinetic response in mixtures of type A and B, revealing that it is coincident with that obtained for the solvatochromic process:[14c] the critical state is preferentially solvated by the structure formed by intersolvent hydrogen-bonded species. In contrast, the reactions carried out in mixtures of type C manifest a tendency to be preferentially solvated by co-solvent $CHCl_3$.
9. The 2,6-DNFB + PIP reactive system in EAc–AcN mixtures constitutes the only example of an *ideal system*. This result can be attributed to a combination of factors related to the substrate structure, the nucleophile structure and the binary solvent mixture properties.
10. Comparing the kinetic response patterns corresponding to the three amines in systems A, B and C, it can be observed that the response obtained in mixtures with $CHCl_3$ is clearly determined by the solvent mixtures, i.e. it is solvent dependent, whereas that corresponding to mixtures with AcN as co-solvent is nucleophile dependent.

EXPERIMENTAL

2,6-DNFB was synthesized as reported previously.[15] PYR and PIP were refluxed for 3 h and then fractionated over sodium. The solvents were purified as usual[14] and all of them were kept over 4 Å molecular sieves and stored in special vessels that allow delivery without air contamination. All binary mixtures were prepared prior to use and stored under anhydrous conditions.

The kinetics of the reactions were studied by UV–visible spectrophotometry. A Perkin-Elmer Model 124 spectrophotometer was used, equipped with a data-acquisition system.

The parameters of solvation which minimize the square residuals of the k_A values were computed by non-linear regressions using the MATLAB 5.2 program.

Acknowledgements

We are indebted to the Universidad Nacional del Litoral (UNL), República Argentina. This work received financial support from the Science and Technology Secretariat, UNL, CAI + D Program (Projects 2000-17-151, 2002-21-152 and 2002-21-153).

REFERENCES

1. Mancini PM, Fortunato G, Adam C, Vottero LR, Terenzani AJ. *J. Phys. Org. Chem.* 2002; **15**: 258–269.
2. (a) Balakrishnan S, Easteal AJ. *Aust. J. Chem*. 1981; **34**: 933–941; (b) Dohnal V, Costas M. *J. Solution Chem*. 1996; **25**: 635–656; (c) Reimers JR, Hall LE. *J. Am. Chem. Soc.* 1999; **121**: 3730–3744.
3. Mancini PM, Pérez AdelC, Vottero LR. *Phys. Chem. Liq.* 2003; **41**: 45–54.
4. Terrier F. *Nucleophilic Aromatic Displacement*. VCH: Weinheim, 1991.
5. Nudelman NS. In *The Chemistry of Amino, Nitroso, Nitro and Related Groups*, Patai S (ed). Wiley: Chichester, 1996; chapt. 26.
6. Crampton M. In *Organic Reaction Mechanisms*, Knipe AC, Watts WE (eds). Wiley: Chichester, 1996; chapt. 5.
7. Fortunato GG. Doctoral Thesis, Facultad de Ingeniería Química, Universidad Nacional del Litoral, Argentina, 2002.
8. (a) Dewar MJS, Zoebisch EG, Healy EF, Stewart JJP. *J. Am. Chem. Soc.* 1985; **107**: 3902–3909; (b) Dewar MJS, Dieter KM. *J. Am. Chem. Soc*. 1886; **108**: 8075–8086; (c) Stewart JJP. *J. Comput. Aided. Mol. Design.* 1990; **4**: 1–105.
9. Bunnett JF, Sekiguchi S, Smith LA. *J. Am. Chem. Soc.* 1981; **103**: 4865–4871.
10. Consiglio G, Arnone C, Spinelli D. *J. Chem. Soc., Perkin Trans. 2* 1982; 721–724.
11. (a) Albert A, Serjeant EP. *The Determination of Ionization Constants.* Chapman and Hall: London, 1971; (b) Hall HK, *J. Org. Chem.* 1964; **29**: 3135–3138.
12. Kamlet MJ, Abboud J-L M, Taft RW. *J. Am. Chem. Soc.* 1977; **99**: 6027–6038, 8325–8327.
13. (a) Bosch E, Roses M. *J. Chem. Soc., Faraday Trans.* 1992; **88**: 3541–3546; (b) Rosés M, Ràfols C, Ortega J, Bosch E. *J. Chem. Soc., Perkin Trans. 2* 1995; 1607–1615; (c) C. Ràfols C, Rosés M, Bosch E. *J. Chem. Soc., Perkin Trans. 2* 1997, 243–248.
14. (a) Mancini PM, Terenzani AJ, Adam C, Pérez A, Vottero LR. *J. Phys. Org. Chem.* 1999; **12**: 713–724; (b) Mancini PM, Terenzani AJ, Adam C, Pérez A, Vottero LR. *J. Phys. Org. Chem.* 1999; **12**: 207–220; (c) Mancini PM, Adam C, Pérez A, Vottero LR. *J. Phys. Org. Chem.* 2000; **13**: 221–231.
15. Parker RE, Read TO. *J. Chem. Soc.* 1962; 3149–3153.

Copyright © 2004 John Wiley & Sons, Ltd.